Fuel 304 (2021) 121450

Contents lists available at ScienceDirect

Fuel

journal homepage: www.elsevier.com/locate/fuel

Impact of flash boiling multiple injections timing on the combustion and thermal efficiency of a gasoline direct injection engine under lean-burn

Zhe Sun [a], Qinglin Xu [a], Mingli Cui [a], Mohamed Nour [a,b], Xuesong Li [a], David L.S. Hung [a,c], Min Xu [a]

[a] School of Mechanical Engineering, Shanghai Jiao Tong University, Dongchuan Road 800, Shanghai 200240, China
[b] Mechanical Engineering Department, Benha Faculty of Engineering, Banha University, Benha 13512, Egypt
[c] University of Michigan-Shanghai Jiao Tong University Joint Institute, Shanghai Jiao Tong University, Dongchuan Road 800, Shanghai 200240, China

ARTICLE INFO

Keywords:
Flash boiling injection
DISI engine
Optical engine
Combustion
Lean burn
Flame diagnostics

ABSTRACT

Lean burn mode of direct injection spark ignition engines (DISI) can improve the engine's thermal efficiency. However, it showed slow flame propagation and combustion instabilities which are strongly related to mixture distribution. Multiple injections can improve control over in-cylinder charge distribution and consequently on burn mode. Additionally, multiple injections can reduce spray impingement and enhance the turbulence in the compression stroke, particularly with late injection, but the time is not enough for spray evaporation. Fuel injection under flash boiling conditions boosts fuel vaporization and spray-airflow interaction of the late injections. This study investigates the effect of flash boiling multiple injections on the combustion of lean gasoline/air mixture in an optical DISI engine. This work uses Mie scattering, CFD, high-speed imaging, and flame images postprocessing model to investigate spray characteristics, spray-airflow interaction, flame propagation, and CH* digital intensity. The results reveal that flash boiling multiple injections has significantly mitigated the liquid spray intensity indicates the elevated rate of vaporization with reduced spray impingement and better interaction with the tumble flow compared to the subcooled single injection. The optimal engine performance and combustion were achieved when the second injection and highest tumble ratio point were timely synchronized, for example, 260°bTDC at 800 rpm and 280°bTDC at 1500 rpm. Thus, flash boiling multiple injections can effectively enhance the thermal efficiency by 54.65% and 11%, respectivly. The CH* digital intensity and heat release showed that flash boiling multiple injections could effectively improve the lean-burn operation of the DISI engine.

1. Introduction

Gasoline direct injection (GDI), also known as direct injection spark ignition (DISI), is a primary technology used in passenger car engines. DISI engine has lower fuel consumption, lower emissions, and better control of the combustion process. However, DISI engines face technical problems such as poor fuel–air mixing, super knock, and spray impingement, leading to pool firing, lower thermal efficiency, and higher PM and NO_x emissions [1]. Several engines and combustion control strategies have been investigated to potentially mitigate the previous concerns and optimize the DISI engine efficiency and reduce emissions. Among various advanced combustion strategies, lean burn combustion (LBC) aims to revolutionize engine thermal efficiency by enhancing high-pressure efficiency, reducing gas exchange losses, and extending the LBC to higher load operation. In addition, LBC can limit the heat transfer losses by lowering the combustion temperature, thereby further improving the thermal efficiency and reducing exhaust pollutants such as NO_x. However, lean mixtures have lower laminar flame speeds, leading to longer combustion duration, decreasing thermal efficiency.

Additionally, LBC in DISI engines may have a higher cyclic variation due to ignition difficulties of lean mixture zones around the spark plug. Therefore, researchers suggested several methods to overcome these difficulties. First, a high-energy ignition system was used to initiate the flame kernel. Secondly, they enabled stratified charges to overcome ignition challenges. The latter was suggested based on the control of the in-cylinder air/fuel mixture through multiple injections to achieve stratified charges[2]. Finally, late injection creates a rich fuel/air mixture around the ignitor while keeping lean fuel/air mixtures near the cylinder liner for general LBC condition and decreasing heat losses at the

E-mail address: xuesonl@sjtu.edu.cn (X. Li).

https://doi.org/10.1016/j.fuel.2021.121450
Received 7 June 2021; Received in revised form 12 July 2021; Accepted 13 July 2021
Available online 20 July 2021

cylinder wall [2].

Multi-injection (or split injection) is the method used to achieve stratified charges by enables fuel injection multiple times during the cycle, and this technique is commonly seen in recent DISI engines. The primary advantage of multiple injection schemes is that multiple injection schemes can reduce each injection's penetration, therefore reducing the likelihood of spray impingement and consequential pool fires, thus reducing the particulate matter emissions from the engines [3]. Also, multiple injection schemes would yield spray plumes with high momentum. The spray carrying more momentum would have a more substantial impact on the in-cylinder airflow field and potentially compromise the turbulence level inside the cylinder. Thus, it would promote the combustion of the engine [4]. However, late liquid fuel injection to achieve charge stratification may cause improper in-cylinder fuel/air mixing with likely impingement on piston or liner. Therefore, there would be some difficulties controlling charge distribution over the whole range of engine operation plus the higher concentration of soot and HC formation at light loads. However, it is possible to overcome such drawbacks using some flash boiling spray technology.

Flash boiling atomization is also a potential approach for generating desirable sprays for the engines of the next generations [5]. Injecting fuels under flash boiling conditions is to vaporize liquid fuel in or out of the injector nozzle by achieving the superheating conditions through low pressure and/or high temperature. A bubble-like two-phase flow is developed, and the fuel droplet evaporation rate is enhanced, and fuel breakup and atomization are improved [6]. The fuel droplet diameter decreased significantly with increasing fuel temperature under flash boiling conditions [7,8]. Meanwhile, some undesirable effects such as spray collapse and injector tip wetting could occur [9,10]. However, spray collapse or injector tip wetting were not confirmed under LBC engine operation. Previous studies about the flash boiling spray reported improved atomization [11] and reduced pool firing [12] for gasoline, biofuels, gasoline surrogates, and single components [13]. Overall, sprays under flash boiling conditions have distinctive characteristics and morphologies compared to subcooled conditions. Such differences are more pronounced under flare flash boiling, under which the breakup process is believed to be dominated by micro-explosions near the injector nozzle exit. We hold that such features of flash boiling atomization might shed lights on innovative combustion systems based on flash boiling atomization, and the benefits of flash boiling combustion have been preliminarily demonstrated in previous optical engine experiments [11,12,14]. It was showcased during the last study that the strong air entrainment characteristics can enhance the fuel–air mixing performance in a constant volume chamber experiment [15]. Furthermore, finer spray droplets reflect a smaller Stokes number due to flash boiling, indicating the spray can easily follow the structured in-cylinder airflow.

Li et al. [16] reported that approaching flash boiling conditions enhanced the atomization and increased the droplet mean velocity. Kale and Banerjee [17] reported that under the flash boiling condition at 423 K, the fuel droplet size reduced by up to 55% compared to its size at 298 K. The result was confirmed by Aleiferis and Romunde [18] for different fuels such as butanol and ethanol at different fuel temperatures and ambient pressures. Serras-Pereira et al. [19] reported that thick film formed by impingement under liquid spray on engine walls could survive for a longer time, while at higher temperatures of flash boiling, the fuel film becomes thinner with a higher rate of evaporation compared to lower temperatures. Knorsch et al.[20] showed that the SMD of fuel droplets reduced by 42.5% when increasing the in-cylinder gas temperatures from 200 °C to 400 °C.

The Micro-LIF-PIV experiment on flash boiling spray showed that the airflow entrainment in flash boiling sprays was enhanced. The momentum of the fuel droplets decreased with a lower Stokes number indicating that the droplets could have a better ability to follow the airflow. Therefore, the fuel atomization and interaction with airflow

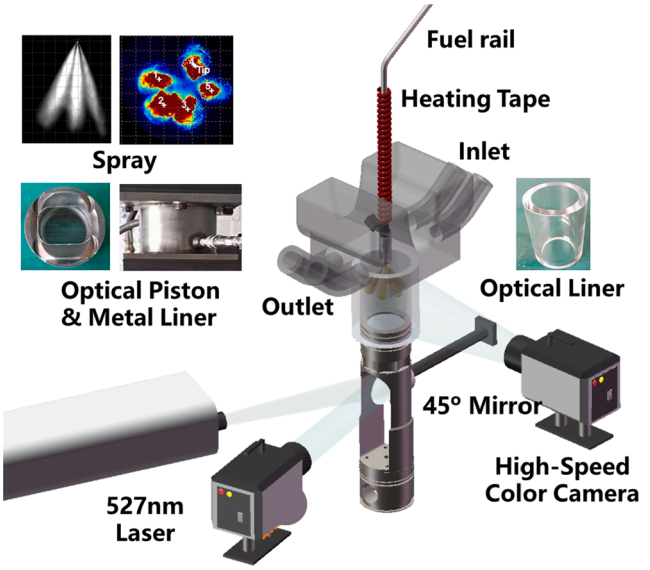

Fig. 1. Experiment of spray and combustion optical diagnostics.

Table 1
Optical engine characteristics and experimental conditions.

Engine specifications	Stroke × Bore	75.1 × 90.3 (mm)
	CR	10.5
	Engine volume	400.17 (cm^3)
	Operating speeds	800, 1500 (rpm)
	Oil/water temperatures	60 (°C)
	Intake pressure	90 kPa
Fuel and injection parameters	Fuel	Gasoline
	RON	92
	Injector	Delphi (GDI), 5 holes
	Rail pressure	10 (MPa)
	Start of injection	Single injection: 300 °bTDC (single) Multiple injection: 1st inj (fixed): 300 °bTDC, 2nd inj (varied): 280, 260, 240, 210, 180, 150, 120 °bTDC
	Injection duration	1900 μs (single, 800), 2500 μs (single, 1500), 950 μs − 950 μs (split, 800) 1250 μs − 1250 μs (split, 1500)
	Injected fuel mass	10.72 mg (800 rpm, single), 5.07 mg/pulse (800 rpm, multiple) 14.29 mg (1500 rpm, single), 6.85 mg/pulse (1500 rpm, multiple)
Ignition conditions	Excess air ratio	1.55 (single) and 1.57 (multiple)
	Spark timing	56 °bTDC (800 rpm), 32°bTDC (1500 rpm)
	Discharge duration	2(ms)

were improved [15]. Additionally, multiple injections promoted the entrainment in flash boiling spray, and results showed that spray has a more substantial impact on the airflow and promotes atomization [15]. This study preliminary investigated the fundamental characteristics of flash boiling multiple injections and showed that flash boiling spray has a unique spray structure and fuel–air interaction mechanisms. However, there is limited to no information considered the effect of the flash boiling multiple injection timing on spray characteristics and subsequent combustion in the DISI engine.

The above review shows the potential of the flash boiling spray technology to improve the performance and combustion of DISI engines. However, limited research discussed the effects of flash boiling multiple injection timings and the interaction with the in-cylinder flow on the combustion mechanisms of the DISI engines under actual operation

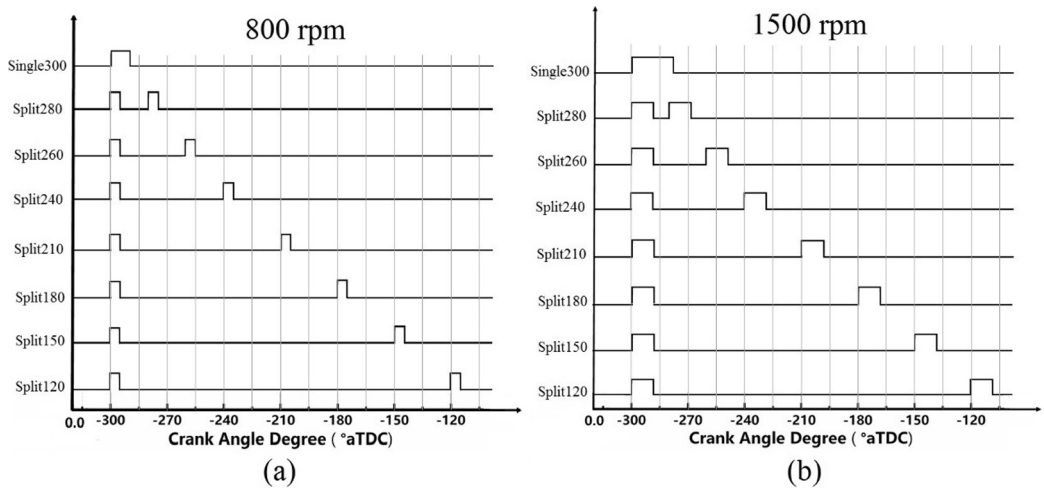

Fig. 2. The tested injection timings and durations at (a) 800 rpm and (b) 1500 rpm.

parameters. Multiple flash boiling injections could provide several advantages, such as boosting the air–fuel mixing and reduce piston/wall wetting by splitting the injected fuel mass into two times and controlling the second injection timing. This provides the primary motivation to perform this study at a wide range of injection timing and engine speed to further optimize the working condition and reach a general conclusion. This study investigated various flash boiling multiple injection timings at different tumble ratios on the DISI engine under LBC, and its influence on the engine's thermal efficiency and flame propagation at different speeds using several experimental and numerical approaches employed in this research.

2. Methodology

2.1. Optical engine

This experiment was conducted using a single optical cylinder based on a spark ignition direct injection engine. The layout of the experimental systems is summarized in Fig. 1. Table 1 presents the engine specifications and experimental conditions. An AVL dynamometer controlled the engine at 800 and 1500 rpm. Also, an AVL cooling and lubricant oil unit maintained the oil and water temperatures at 60 °C (±1°C). The coolant temperature of 60 °C was more appropriate to study the effects of flash boiling atomization during the engine warming up process, therefore it was adopted in this study, and such a temperature was also selected in others' investigations [21]. Meanwhile, at higher coolant temperatures of 90 °C, the spray tends to be under transitional flash boiling conditions [22–24]. Excessive water temperature will heat the fuel and make the spray at transient flash boiling conditions, and lower temperature will lead to being different from the actual working condition. Various configurations were used to realize the in-cylinder spray, flame propagation, and pressure analysis. For spray investigation, the optical liner and optical piston were used to record the spray scattering signal. The plume structure and targeting from the five-hole GDI Delphi injector are presented in Fig. 1. The fuel rail pressure was 10 MPa, and the backpressure was 40 kPa. The laser pulses from the high-speed Nd: YLF laser (527 nm) with 10 kHz pulse frequency were reflected into the engine cylinder using a 45° mirror installed below the optical piston. The spray scattering signal was recorded for 20 successive cycles using a high-speed color camera. The imaging frequency was 6 Kfps at 384 × 632 pixels.

A spark plug with a high energy of 826 mJ and a discharge duration of 2 ms ignited the lean fuel–air mixture with lambda of 1.55 and 1.57. The in-cylinder flame was filmed based on the Bowditch method utilizing the high-speed color camera, quartz piston, and bottom accessed45^{o}-mirror. The combustion images were captured at 6 Kfps with 150 recoded images per cycle at a spatial resolution of 332 × 332 pixels. The piezoelectric pressure transducer from Kistler was placed at the cylinder head, and the combustion analyzer (AND) recorded the cylinder pressure each 0.1 CAD for 100 successive cycles. The engine control unit is used to adjust the start of injection and ignition timing. Also, signals from the pressure transducer and high-speed camera were timely synchronized. For instance, the combustion imaging started when the ignition signal was given. A heating tape, thermocouple, and controller adjusted the fuel temperature at subcooled or flash boiling conditions. The fuel temperatures were adjusted to 30 °C and 200 °C for subcooled and flared flash boiling conditions. This setting allows for a flare flash boiling condition of most of the gasoline components. The injection strategies, including the duration and injected masses are summarized in Table 1, while the injection and ignition timings are described in Fig. 2. The injection conditions of single subcooled, single flash boiling, multiple subcooled, and multiple flash boiling have been denoted SS, SF, MS, and MF.

The single injection timing is fixed at 300°bTDC and denoted as SS300 and SF300 for single subcooled and flash boiling cases. In multiple injections, the 1st injection timing is kept at 300°bTDC, while the 2nd injection timing varied as indicated in Table 1 and Fig. 2. The multiple injection conditions are denoted as MF210 and MS210 for flash boiling and subcooled, and 210 indicates that the 2nd injection timing is at 210°bTDC. The dwell-time between the first and the second injections was selected to avoid effects from the first injection on the second injection, which could result due to rail pressure fluctuation and hydrodynamic behavior of the injector valve. Therefore, the shortest dwell-time between injections was 2.22 ms and 0.95 ms for MS280 cases at 1500 and 800 rpm, respectively, while it takes 0.5 ms for the injector dynamic flow to become stable. The spark timings of 56 °bTDC and 32 °bTDC for 800 rpm and 1500 rpm, respectively, were selected for the MBT point for the single injection case. The experimental conditions are presented in Table 1.

2.2. Cylinder pressure and heat release analysis

Liu and Dumitrescu [25,26] suggested a methodology developed for combustion analysis started by a spark ignition in a diesel bowl geometry using the derivatives of AROHR. The first and second derivatives of AROHR represents its variation at different stages. The first derivative of the AROHR determines how much the ROHR increased or decreased. The positive slope of the first derivative of AROHR indicates a rise in the value of AROHR, while a negative slope denotes a reduction in its value. However, the physical meaning of the second derivatives of AROHR is

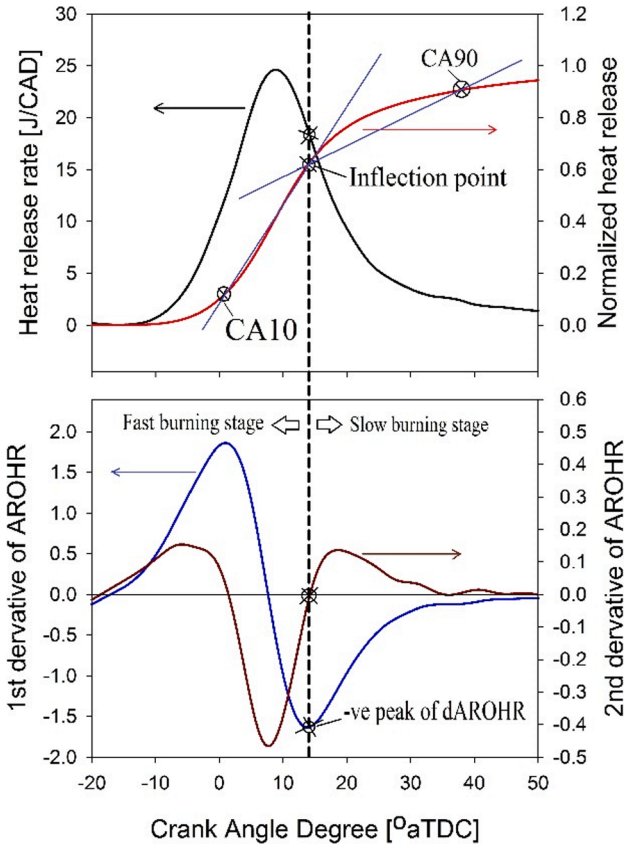

Fig. 3. Sample of combustion and heat release analysis.

not clear and can be used as a mathematical way to quickly distinguish the combustion phase and find the inflection point. The fast-burning stage around the TDC has a better thermal efficiency from the thermodynamic perspective. The CA at which the first derivative of AROHR attains a negative peak and the CAD at which the second derivative equals zero are considered the end of the fast-burning process and the start of the slow-burning process. A vertical line is drawn from the negative peak of the first derivative of AROHR and to the CA at which the second derivative is equal to zero, as shown in Fig. 3. It connects points on the curves of the first derivative, second derivative, CA, AROHR, and normalized heat release (NHR). The intersection of the vertical line, NHR, and AROHR curves represents the inflection point. It is evident from the NHR curve that the burning rate and the slope of the NHR curve changed before and after this point. This is demonstrated in Fig. 3(a) by connecting CA10 to the inflection point (IFP) and connecting the IFP to CA90. This point was considered as a transitional point from the fast-burning mode to the slow-burning mode in the study reported by Liu and Dumitrescu [25,26]. They observed that the flame spreading and flame front areas within the piston bowl were higher than those during the subsequent combustion process occurring in the squish region. Consequently, the burn rate undergoes a drastic change about the inflection point, as seen in Fig. 3(a) [25,26]. The parameters analyzed in the combustion phasing of this study include CA10 (SOC), IF (separate fast and slow burn rates), CA50, and CA90 (EOC). The ID, combustion duration, and fuel fractions were then calculated during the slow-burn and fast-burn modes.

2.3. Flame images postprocessing

In the flame, the self-luminescence of various excited free radicals makes the flame present the main components of different pops in the spectrum. These components dominate the structure of the entire flame and show different colors in the color camera. OH*, CH*, C2* are the main products of the hydrocarbon fuel-dominated combustion flame diffusion in DISI, and its band position will not fluctuate significantly with the air–fuel ratio [27]. Regarding the main reaction area of combustion, heat release represents the primary functional transformation of chemical reactions, which is very important in the thermodynamic cycle of the engine. Studies have shown that several emissions can reflect the position of exotherm to a certain extent and become HR markers [28,29]. CH* can be used as an effective product representing the exothermic position in the visible light range. In the simulation based on chemical reaction kinetics, the distance from the exothermic position is between 70 μm and 130 μm, and by increasing the pressure (greater than 1 bar), the space continues to shrink. In the optical engine flame test, the camera's resolution is 139 μm/pixel, which means that this scale can be well applied in our test system, and CH* can indicate the heat release. A unique digital image processing method was used to analyze the flame image based on a color camera as shown in Fig. 4. The flame image processing model for C2*, CH*, and premixed flame was built and discussed in detail in our previous research [14], while the basis of the postprocessing color model to characterize flame properties are summarized in Fig. 4(a). First, the RGB response of this color camera was as follows. Below the blue filter 400 nm, its response is relatively low, and there is no good response in the peak band of OH*, which restricted the ability to obtain the flame amplifier directly. The CH* that dominates the blue band can be calculated separately. In the test based on the diffuse combustion flame light source with a spectrometer, it was found that the influence of C2* in the blue band on CH* is controlled below 40%, and the intensity of CH* is near the response peak of the blue filter. Considering the impact of line of sight and accuracy in the optical engine, although this method cannot fully represent CH*, it can be regarded as to extract a more accurate "dark blue" to describe CH* to a certain extent, thereby obtaining a representative result of heat release distribution (HR MARKER). This result is also compared and coupled with the heat release result based on cylinder pressure in the following text. It also proves that it has a certain accuracy and has strong application potential. It can quickly and efficiently understand and analyze the continuous high-speed combustion process without losing the original picture. The raw image is the original image from the camera with the binary denoising [30]. The color model processing method can extract the premixed flame very well, as discussed in our previous study [14], but this was for stoichiometric combustion, and a completely mixed flame structure can be obtained. When CH* is separated, the main heat release area of the flame can be identified qualitatively. This area is not completely uniform and symmetrical during the flame diffusion process of the engine, but the concentration distribution and size contrast can be seen.

2.4. Simulation of in-cylinder airflow

The in-cylinder airflow was simulated using CFD. The CFD work was conducted using CONVERGE software. The engine 3D geometry was imported, the boundary conditions were set, and the engine surface mesh model was generated. To balance the calculation time and accuracy, the basic size of the volume grid was set to 8 mm, the in-cylinder grid was embedded by level 2, and the inlet and exhaust valve zone were embedded by level 3. The adaptive speed grid densification level was 3. The total number of cells is 24230 ~ 80477. Fig. 5 shows the computational domain and meshing. The turbulence model was set as RNG k-ε. The timing was calculated from the start of intake stroke to the TDC without applying spray and combustion models.

The tumble ratio was calculated based on the CFD simulation, and the relationship between the tumble ratio and the injection timing is shown in Fig. 6. The change of tumble ratio with CAD at 800 rpm and 1500 rpm is indicated in Fig. 6. The high tumble ratio is shown between 280 and 240 °bTDC, and the air-spray interaction during these CAD could be the highest. Fig. 6 shows the comparison between different injection timings concerning the air-spray interaction, fuel vaporization

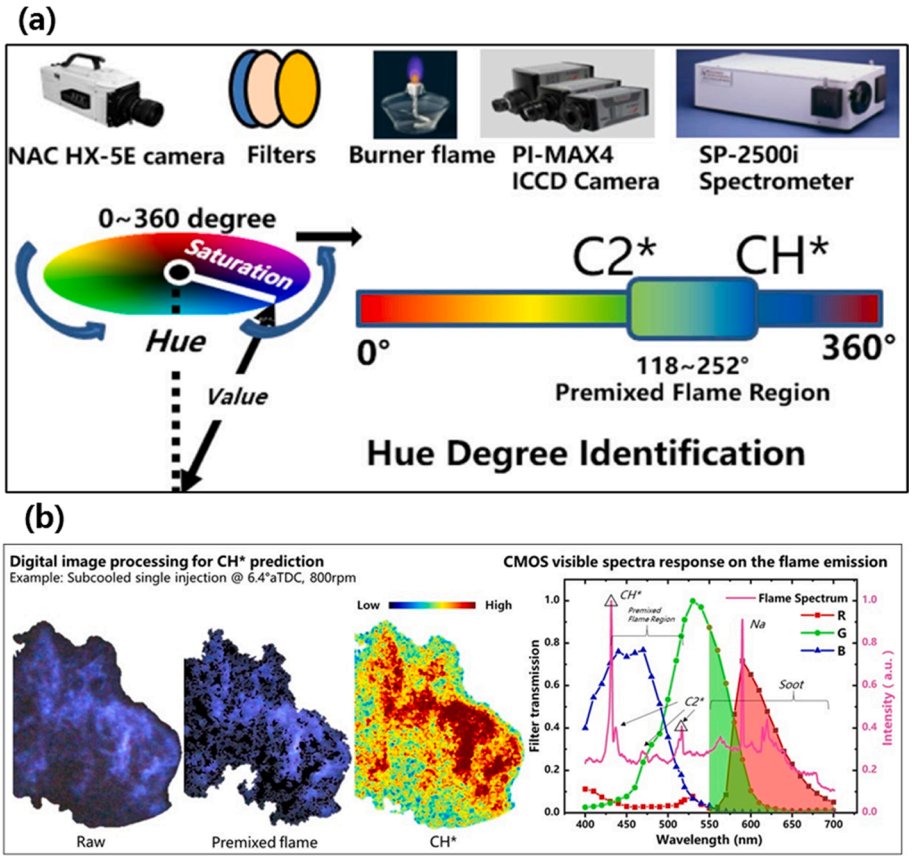

Fig. 4. Flame image postprocessing (a) overview and basics of the postprocessing color model to characterize flame properties (b) sample of CH* and premixed flame identification from the raw flame image.

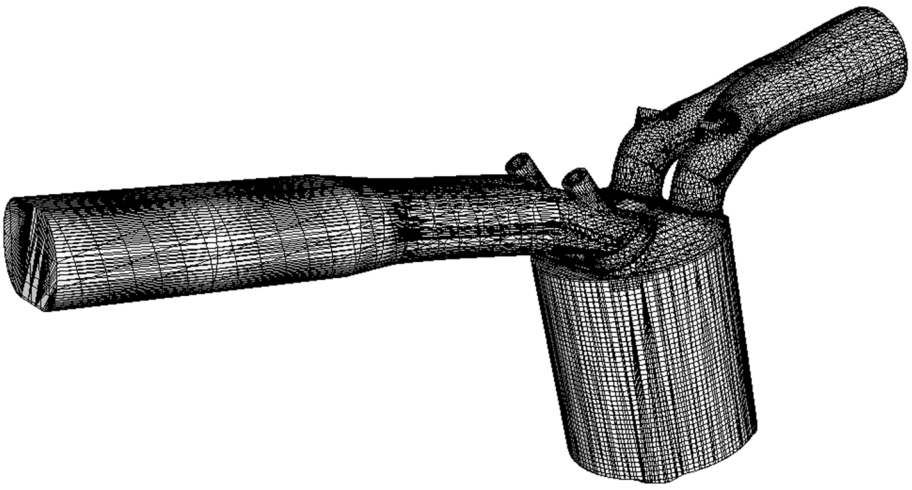

Fig. 5. Computational domain and meshing for in-cylinder airflow structure simulation.

level, and impingement level. The injection timing can control the interaction among spray impingement, air–fuel interaction, and evaporation. When the injection timing is set to be during the earlier stage of the intake stroke and the later stage of the compression stroke, the possibility of spray impingement and piston wetting is high. Meanwhile, the split injection could reduce this possibility due to the reduced penetration. Also, when the second injection timing is set to be at the point of the highest tumble ratio, the higher momentum will lead to the local spray-induced flow and enhance the mixing. In addition, earlier and later injection timings will lead to the variation of the evaporation time. Therefore, the most appropriate injection timing and injection strategy could be achieved by getting the best result based on optimizing these factors. It is worth noting that in-cylinder PIV measurements also validated this model to ensure the accuracy of the tumble ratio calculation.

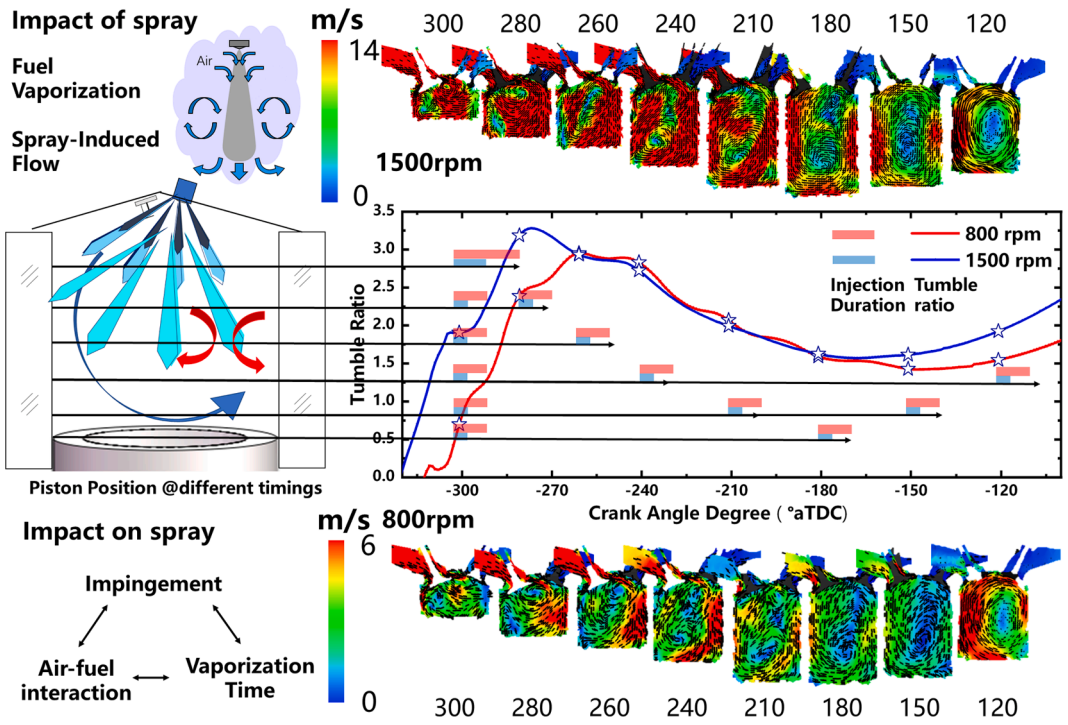

Fig. 6. In-cylinder airflow and relation with injection timing.

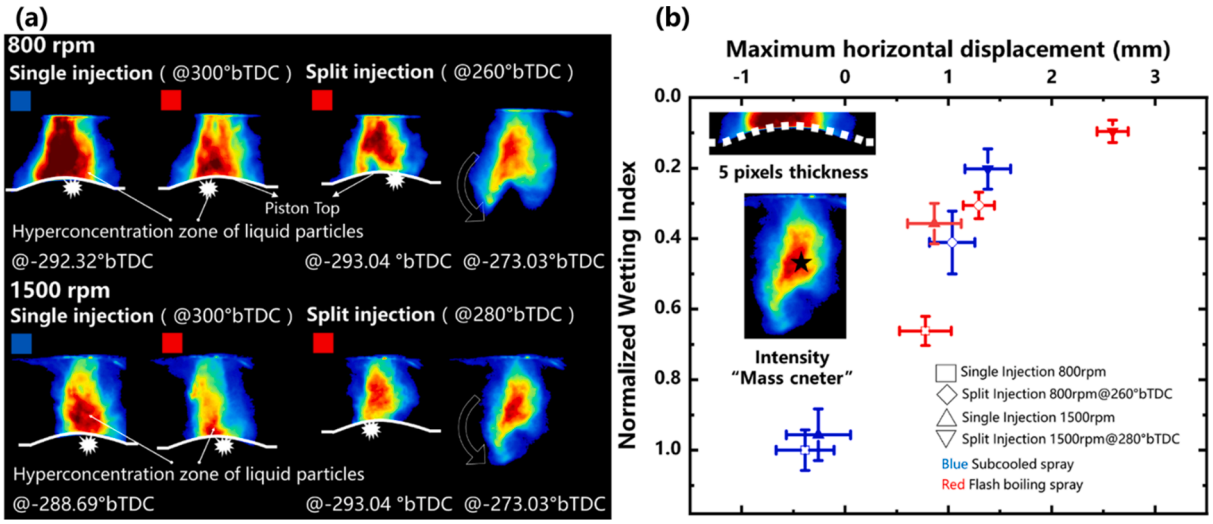

Fig. 7. Comparison under different (blue) subcooled and (red) flash boiling conditions: (a) spray process and (b) wall wetting and spray displacement analysis. (For interpretation of the references to color in this figure legend, the reader is referred to the web version of this article.)

3. Results and discussion

3.1. Spray morphology

The subcooled and flash boiling spray morphology for single and multiple injections at different speeds of 800 and 1500 rpm are illustrated in Fig. 7(a). The shown images present the probability of spray concentration and distribution in-cylinder, and it is attained from twenty injections. Therefore, the cyclic variations of spray structure can be shown. The strength of the scattered signals indicates the concentration of the liquid droplets, which qualitatively depicts the difficulty of the charge mixing process and the possibility of more rich regions. This is a qualitative analysis of spray structure under subcooled or flash boiling parameters. Fig. 7 shows that all sprays were collapsed either for subcooled or flash boiling conditions. Spray collapse is a well-known effect of flash boiling conditions. However, it is also observed for subcooled in this test. This could be attributed to the warm engine operation as the coolant temperature was controlled around 60–70 °C and the low in-cylinder pressure of 0.5 bar during injection and the effect of the high in-cylinder tumble flow variations. The same results were also reported in the literature [31,32].

However, the liquid phase scattering intensity for SS300 at 800 and 1500 rpm was stronger than SF300. Also, it was higher than the MF260 at 800 rpm and MF280 at 1500 rpm, as shown in Fig. 7(a). The area of the red zone at the center of the spray is more prominent, which means that more liquid droplets are concentrated at the center under subcooled conditions. Meanwhile, the flash boiling condition boosted the fuel vaporization and showed the less red area and more turquoise, yellow,

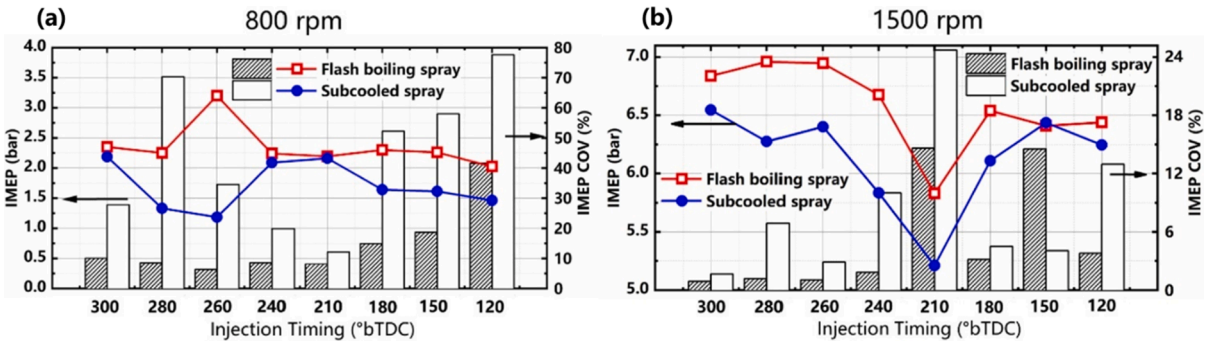

Fig. 8. Variation of IMEP and COV under different injection timing, fuel temperature at (a) 800 rpm and (b) 1500 rpm.

and blue areas, which means less liquid phase and more vapor phase. Recent literature also showed that injecting fuels under flash boiling conditions enhanced atomization[11], reduced droplet size, decreased impingement[33], lowered soot [34], and mitigated pool firing [12].

The spray impingement on walls may form fuel films that reduced fuel–air homogeneity and leads to pool firing and enhance soot formation. Fig. 7(a) shows that under multiple flash boiling injection cases (MF260 and MF280), the total injected fuel mass per cycle was divided into two halves, and each split injection injects only 50% of the total fuel mass. Therefore, the spray penetration at the first injection at −293 °aTDC reduced, and spray impingement decreased. Also, applying the flash boiling spray to multiple injections helped to reduce the spray impingement on the piston top surface. The contact line between the piston top surface and the red zone was longer for the SS300 case than the SF300 case, reflecting the substantial impingement. However, the second injection at −273 °aTDC showed a different spray structure, which has taken the shape of the tumble flow structure more. This is mainly attributed to the injection timing of the second injection. Additionally, the contact line between the spray and engine top surface was not shown during the second injection due to the lower piston position and less spray penetration, reflecting the complete prevention of spray impingement for half of the injected fuel mass. The shown conditions for the spray are MF260 and MF280 because they correspond to the highest values of tumble ratios variation at 800 and 1500 rpm, as shown in Fig. 6. Therefore, the flash boiling multiple injection spray structure interacted with the tumble flow giving a better air–fuel mixing process than single injection cases.

For further analysis of spray impingement, Fig. 7(b) shows the variation of the normalized wetting index versus the maximum horizontal displacement. The wetting index was calculated by identifying the piston's surface and summing the spray intensity within 5 pixels thickness boundary above that accumulated during the entire process of impingement. The maximum horizontal displacement is the intensity "mass center" of spray in the x-direction during the spray process, representing the effect of the airflow on the spray. The wetting index was significantly reduced under SF injection conditions compared to SS spray. At the same time, a further reduction occurred under flash boiling multiple injection conditions. Fig. 7(b) shows that the multiple injections flash boiling spray can reduce the amount of wall wetting by up to 90%, and the spray can be bent by 2.5 mm, which is increased by more than 60% compared to SS injection. This reflects the significant improvements from multiple injection flash boiling spray.

3.2. Performance analyses

The cylinder pressure of 100 cycles was recorded, and the IMEP and COV_{IMEP} were calculated. As shown in Fig. 8, there are eight cases in comparison, including the single injection case and seven multiple injection cases as described above. The values of IMEP are ranged from 1 to 2.2 bar and 2.2 to 3.3 bar for different subcooled and flash boiling spray cases at 800 rpm. Meanwhile, the values of IMEP are ranged from 5.2 to 6.5 bar and 5.8 to 6.9 bar for different subcooled and flash boiling spray cases at 1500 rpm. Furthermore, Fig. 8 shows that the COV_{IMEP} values are in the range of 10–80% for 800 rpm and 1–24% for 1500 rpm. The high COV_{IMEP} values at 800 rpm were due to the nearly idle condition at this low speed combined with the lean burn. Many lean and ultra-lean burn studies in the literature reported such high COV_{IMEP} values and high cyclic variation, particularly at idle conditions [35–38]. At both tested speeds, the multiple injection cases can be divided into three groups based on second injection timing: early intake stroke injection (280 and 260), late intake stroke injection (240 and 210), and injection during the compression stroke (180, 150, 120). The main differences between these three groups are the level of air–fuel interaction (see Fig. 6), the available time for evaporation, and the spray impingement level on the piston top surface.

At the lower speed of 800 rpm, the IMEP value of MS280 and MS260 decreased by 36% under subcooled conditions compared to SS300. This could be attributed to that under subcooled spray, the early intake stroke injection group (MS280 and MS260) has a slightly shorter time for evaporation, slightly improve air–fuel interaction, and lower spray impingement level compared to the SS300. However, under the flash boiling injection, the IMEP increased compared to the subcooled injection. The IMEP increased by 40% for the MF260 case compared to SF300 at 800 rpm. Under the subcooled condition, the COV_{IMEP} of MS280 and MS260 is higher than that of SS300, which means deteriorated combustion stability. Generally, the COV_{IMEP} decreased under the flash boiling spray for all conditions. This could be attributed to the improved fuel atomization that improves the mixture homogeneity and increases combustion stability.

At 800 rpm, the COV_{IMEP} of MF280 and MF260 was even lower than SF300 under flash boiling conditions. This improvement in combustion stability is because of the self-entrainment around spray plumes that also enhanced by injecting fuel at the highest tumble ratio. There are vortex flow fields around the spray plume, and multiple injections improve this advantage, making fuel distribution and air–fuel mixing better. This phenomenon was experimentally studied in the previous study [15]. The late intake stroke injection cases of MS240, MS210, MF240 and MF210 have almost the same IMEP as the SS300, while no significant change in IMEP occurred under flash boiling conditions. The COV_{IMEP} of MF240 and MF210 cases was lower than SS300 and SF300 cases, and lower than MS240 and MS210, which confirms that combustion stability improved under flash boiling spray.

For the injection during the compression stroke group at 800 rpm, the IMEP of MS180, MS150, and MS120 cases were reduced by 27%, 27%, and 31%, respectively, compared to SS300. This could be attributed to that injection during compression stroke with such low injection pressure may result in deteriorated fuel atomization, short vaporization timing, and piston backpressure, affecting charge formation under the subcooled spray. However, under the flash boiling spray, the IMEP of these cases was almost like SS300 and SF300.

At the high tested speed of 1500 rpm, the IMEP of MS240 and MS210 decreased by 30% and 18%, respectively, compared to SS300. The late

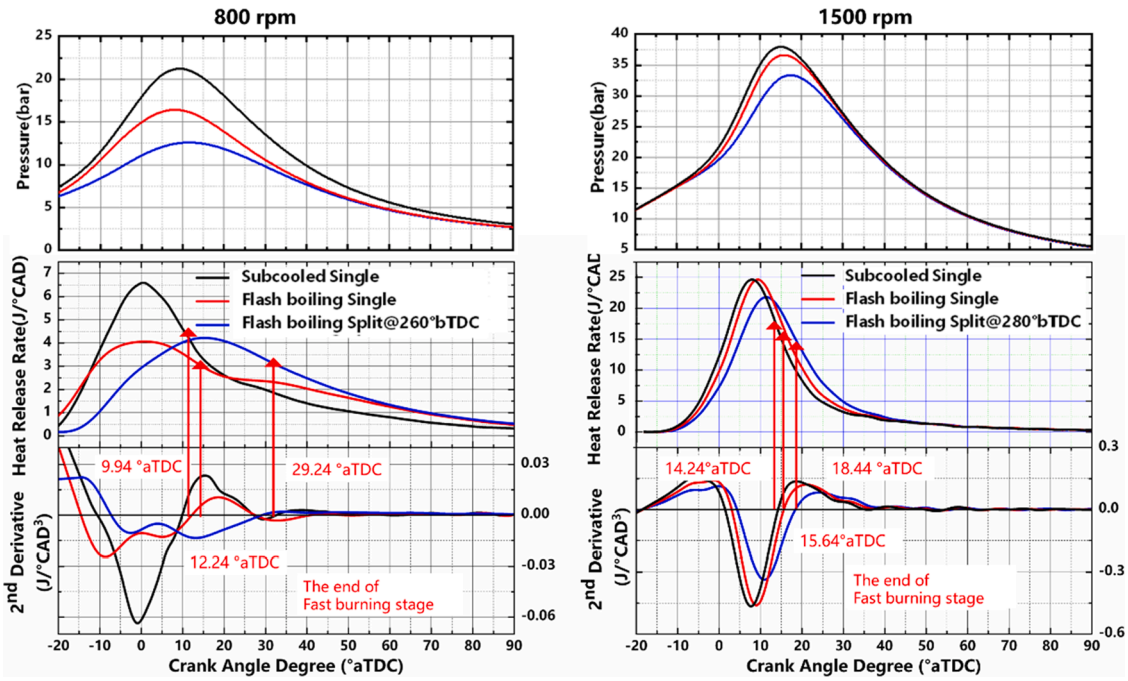

Fig. 9. The heat release rate and its second derivative under different flash boiling multiple injection timing.

intake stroke injection of MS240 and MS210 gives a much shorter time for evaporation and a very low spray impingement level than a single injection at 300 °bTDC (SS300). Meanwhile, the COV_{IMEP} of these cases was significantly more than that of the SS300 case. For flash boiling injection, The COV_{IMEP} decreased (more stable combustion), and the IMEP increased but remained lower than that of SF300. The COV_{IMEP} of MF240 was almost like SF300, while it was much higher for MF210. The sharp decrease in the IMEP of MS210 and MF210 at 1500 rpm compared to MS240 and MF240 could be attributed to the decreased tumble ratio at 210 °bTDC conditions, unlike MF240 improved tumble flow. Additionally, the remaining evaporation timing is short for the second injection, so that the IMEP decreased.

Under flash boiling injection, the IMEP improved but still lower than that of SF300. At 1500 rpm, the IMEP of MS180, MS150, and MS120 reduced by 6.8%, 1.5%, and 4.5%. This could be because the injection during compression stroke group (MS180, 150, 120) has the shortest evaporation time for the second injection, the lowest spray impingement level, and strong airflow with a high tumble ratio compared to the other to SS300. However, in the MF150 and MF120 cases, where the fuel was injected during compression, the spray penetration, breakup, and atomization were affected by in-cylinder pressure increase, and the IMEP and COV_{IMEP} become worse with poor fuel vaporization due to the limited time. Although the airflow is strong enough at MF120 and MF150, the evaporation remaining time plays a more critical role so that more fuel has not been evaporated and an inhomogeneous mixture formed. MF280 and MF260 cases at 1500 rpm and 800 rpm show the highest IMEP and the lowest cyclic variation among all multiple injection cases compared to SS300. This is attributed to the highest tumble ratio at these points with strong air–fuel interaction. Therefore, an overall combustion improvement can be noted.

The heat release rate and its second derivative are shown in Fig. 9 for MS260-800, MF260-800, MS280-1500, MF280-1500, SF300, and SS300. Multiple injections at 260°bTDC and 280°bTDC were selected as they showed the highest IMEP and the lowest COV_{IMEP}. At 800 rpm, MF260 showed a higher heat release rate with a faster burning mode compared to SF300 and SS300. The second derivative of heat release rate indicates that the MF260 has more heat release under fast burn mode than the SS300 case. The SS300 case has a much longer burn phase

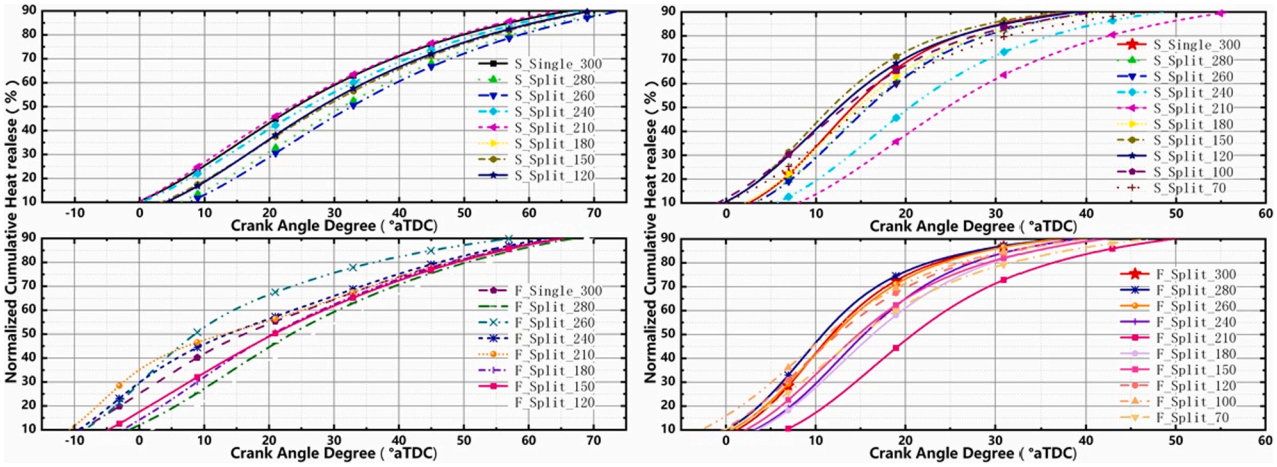

Fig. 10. Variation of normalized heat release under different injection timing, fuel temperature, and engine speed.

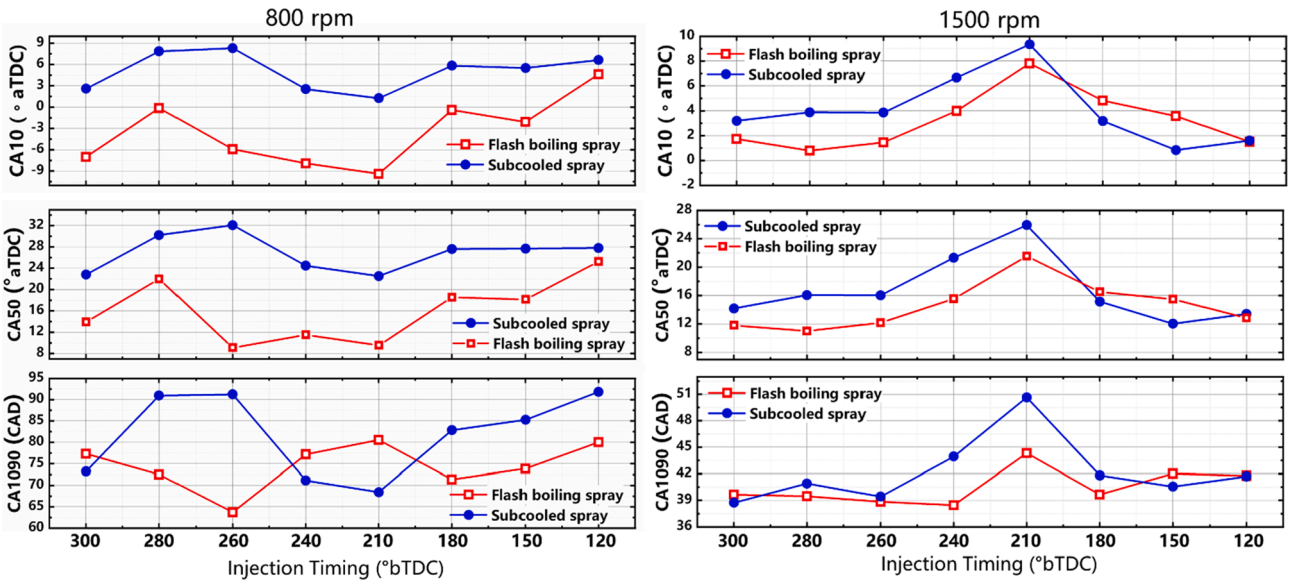

Fig. 11. CA10, CA50, and CA10-90 analysis under different injection timing, fuel temperature, and engine speed.

duration, as in Fig. 9. The end of fast burn mode under the subcooled single spray, flash-boiling single-injection, and multiple flash boiling sprays is 29.24°aTDC,12.24°aTDC, 9.94°aTDC. This means that flash boiling multiple injections is 19.3 CAD advanced compared to the subcooled single spray. This is also clear in Fig. 10 from the normalized cumulative heat release of all conditions. At 1500 rpm, the MF280 case showed the highest heat release rate and the most advanced timing compared to the single injection case under flash boiling or subcooled. The second derivative also shows that MF280 has a faster burn mode compared to SS300 and SF300 cases. The end of fast burn mode under the subcooled single spray, flash boiling single spray, and multiple flash boiling spray is 18.44°aTDC,15.64°aTDC, 14.24°aTDC. This also means that flash boiling multiple injections is 4.2 CAD advanced compared to the subcooled single spray. Thermal efficiency will be enhanced, attributed to the improved fuel–air mixture preparation of multiple injection flash boiling. Additionally, multiple injection flash boiling has a more remarkable improvement on engine performance under lower engine operation speed.

The combustion phasing of different injection cases is presented in Fig. 11. This includes CA10, CA50, and CA90, which are defined as crank angle degrees at which 10%, 50%, and 90% of total heat release, respectively, while CA1090 shows the crank angle degrees between CA10 and CA90. CA10 and CA50 are used to define the start of combustion and the combustion phasing, which are in a similar trend in the tested cases, while CA1090 shows the combustion duration. The results reveal that the regular subcooled multiple injections have a longer delay and retarded combustion phasing (CA10 and CA50). The late injection of 50% of the injected fuel mass at the compression stroke, such as MS/MF150 and MS/MF120 at 800 rpm, leads to a less homogenous mixture formation along with large combustion fluctuations, as seen in Fig. 8. Also, fuel injection during the compression stroke may reduce spray penetration, fuel breakup, and atomization. Besides, the injected fuel mass needs to absorb heat from surrounding gas to vaporize during this short time, which reduces the in-cylinder temperature and delays the start of combustion. However, in the case of MS/MF180, 150, 120 at 1500 rpm, 50% of the fuel mass was injected while the piston at BDC or

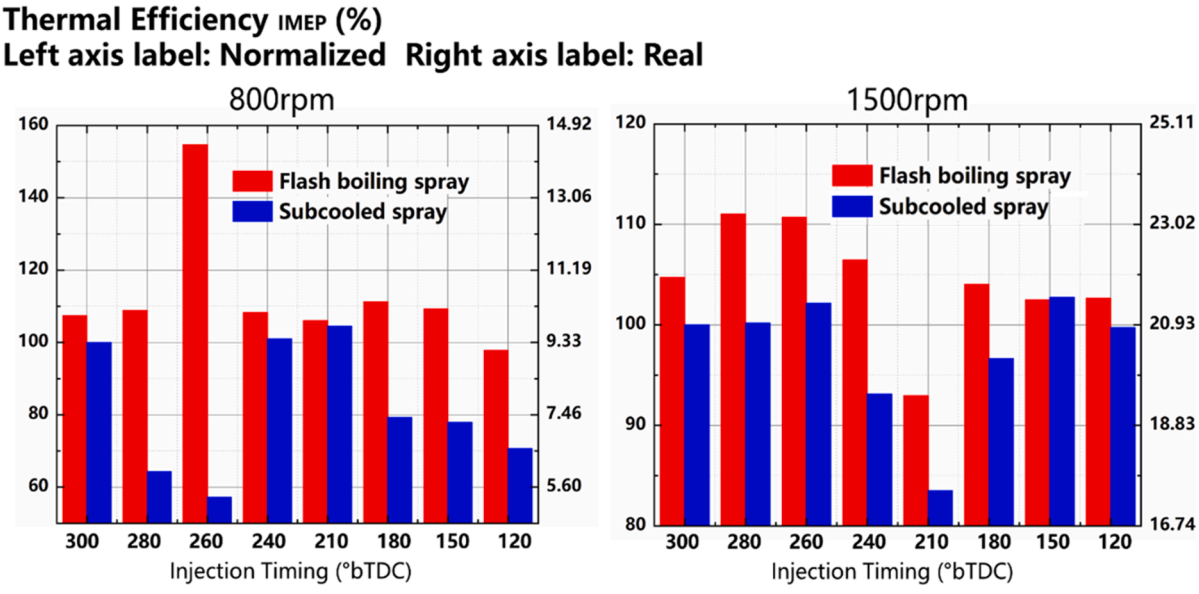

Fig. 12. Normalized and real thermal efficiency under different injection timing, fuel temperature, and engine speed.

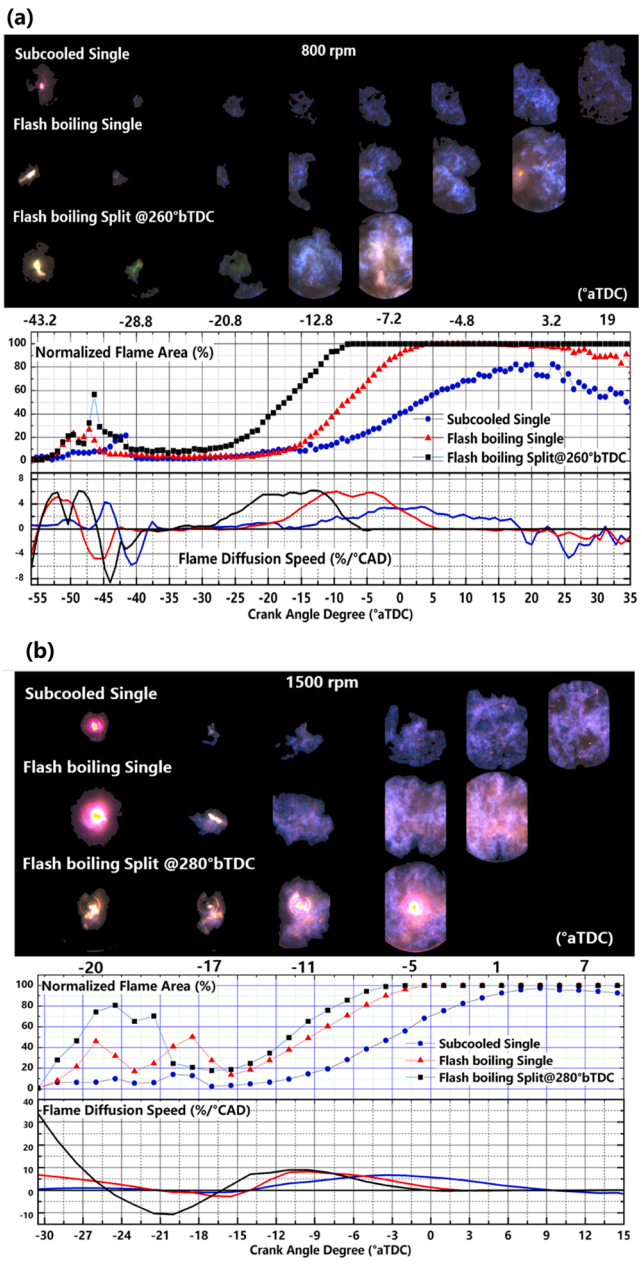

Fig. 13. Flame propagation, normalized flame area, and apparent flame speed under flash boiling and subcooled spray conditions at (a) 800 rpm and (b) 1500 rpm.

during the compression stroke, the durations from ignition to CA10 or CA50 are shortened for these conditions. Although the second injection timing for these conditions is relatively late, the piston position and in-cylinder pressure have a very low effect on the spray penetration and atomization. Also, the airflow at these crank angles has a stronger tumble flow, which promotes fuel distribution and mixture that advanced the combustion timing. This facilitates the initial flame development results in early CA10 and CA50 compared to SS300. Obviously, in MS/MF150 and MS/MF120, the overall combustion duration is longer than MS/MF180. This is attributed to the burn of the remaining unburned mixture at the late phase. The flash boiling multiple injections showed an earlier start of the combustion process as CA10 and CA50 for all-flash boiling conditions were earlier than subcooled. It shows the same trend as the subcooled conditions. Also, the overall combustion duration CA10-90 reduced under flash boiling conditions.

The thermal efficiency was calculated relative to the single-300 subcooled case as shown in Fig. 12. It was calculated by the IMEP and the heat value of the fuel injected. Due to the heat losses and gas leakage in the optical engine test, the calculated thermal efficiency was lower than the actual engine. However, the comparison under different conditions was meaningful. At 800 rpm under the subcooled spray, the thermal efficiency of almost all multiple subcooled injection cases was lower than that of SS300. MS240 and MS210 under subcooled have nearly the same thermal efficiency as SS300, while MS280 and MS260 were the lowest. This low thermal efficiency of MS280 and MS260 is attributed to insufficient stable airflow intensity and the high COV_{IMEP}. At 1500 rpm under the subcooled spray, the thermal efficiency improved for multiple injection conditions such as MS280, MS260, MS150, and MS120, while the thermal efficiency decreased for MS240, MS210, and MS180. Under flash boiling spray conditions at both 800 rpm and 1500 rpm, the thermal efficiency increased. The highest thermal efficiency was for MF260 at 800 rpm and MF280 at 1500 rpm. This is attributed to the improved vaporization and fuel–air mixtures formation under flash boiling conditions.

3.3. *Transient flame propagation*

The flame propagation for the three typical selected conditions to represent the SS, SF, and MF is shown in Fig. 13. Due to the limitation of the optical quartz window, the presented flame images are only before the flame propagates to fill the optical window area. The flame propagation showed two stages. Firstly, the flame kernel formation under the plasma of the high-energy ignition system. Secondly, the self-sustained flame propagation. These stages are clear in Fig. 13 as flame area increased between −55 to −40 aTDC (at 800 rpm) and −30 to −15 aTDC (at 1500 rpm) and then reached again to zero (kernel initiation) before the flame started to propagate (self-sustained flame) again reaching 1. However, the energy diffusion of the igniter requires strong airflow to grow the initial flame core. Therefore, under low-speed engine operating conditions, the ignition process takes a longer duration, and the flame expands more slowly due to the weaker in-cylinder airflow, less fuel mass, along with the lean-burn mode than the higher engine speed. At 1500 rpm, a brighter yellow flame was emitted during the ignition phase due to the high energy system with stronger airflow and fuel–air interaction. The flame propagation at 800 rpm shows that flash boiling conditions showed significantly higher flame spreading rates than subcooled spray. Also, the flash boiling multiple injections improved flame propagation compared to the flash boiling single spray. The flame propagation at 1500 rpm has the same trend as 800 with higher rates and fewer differences between the tested conditions. The multiple injection flash boiling showed faster flame propagation compared to single injection flash boiling or subcooled.

The variation of digital CH* intensity under the three typical selected conditions of SS, SF, and MF is shown in Fig. 14. The digital CH* intensity can be used to indicate the heat release under each condition. The subcooled single injection showed the lowest digital CH* intensity compared to the flash boiling tested conditions. Under flash boiling injection, the digital CH* intensity increased shows a higher heat release. The intensity of CH* is higher under MF conditions is higher than in SF injection cases. The flame images postprocessing shows that the under-flash boiling condition, the digital CH* intensity distribution, and uniformity are better than subcooled. The flash boiling multiple injections also show better digital CH* intensity than the flash boiling single injection.

Fig. 15 presents the variation of the digital CH* intensity and the heat release rate. The digital CH* intensity increased with the increase of the heat release rate and showed the same trend as shown in Fig. 15. The CH* has the same location of the heat release and can be used as an HR marker, as discussed earlier. Therefore, digital CH* intensity can be used to represent the heat release process. Fig. 15 shows that the CH* of MF is higher than that of SF, and the digital CH* intensity of flash boiling cases was higher than that of subcooled cases.

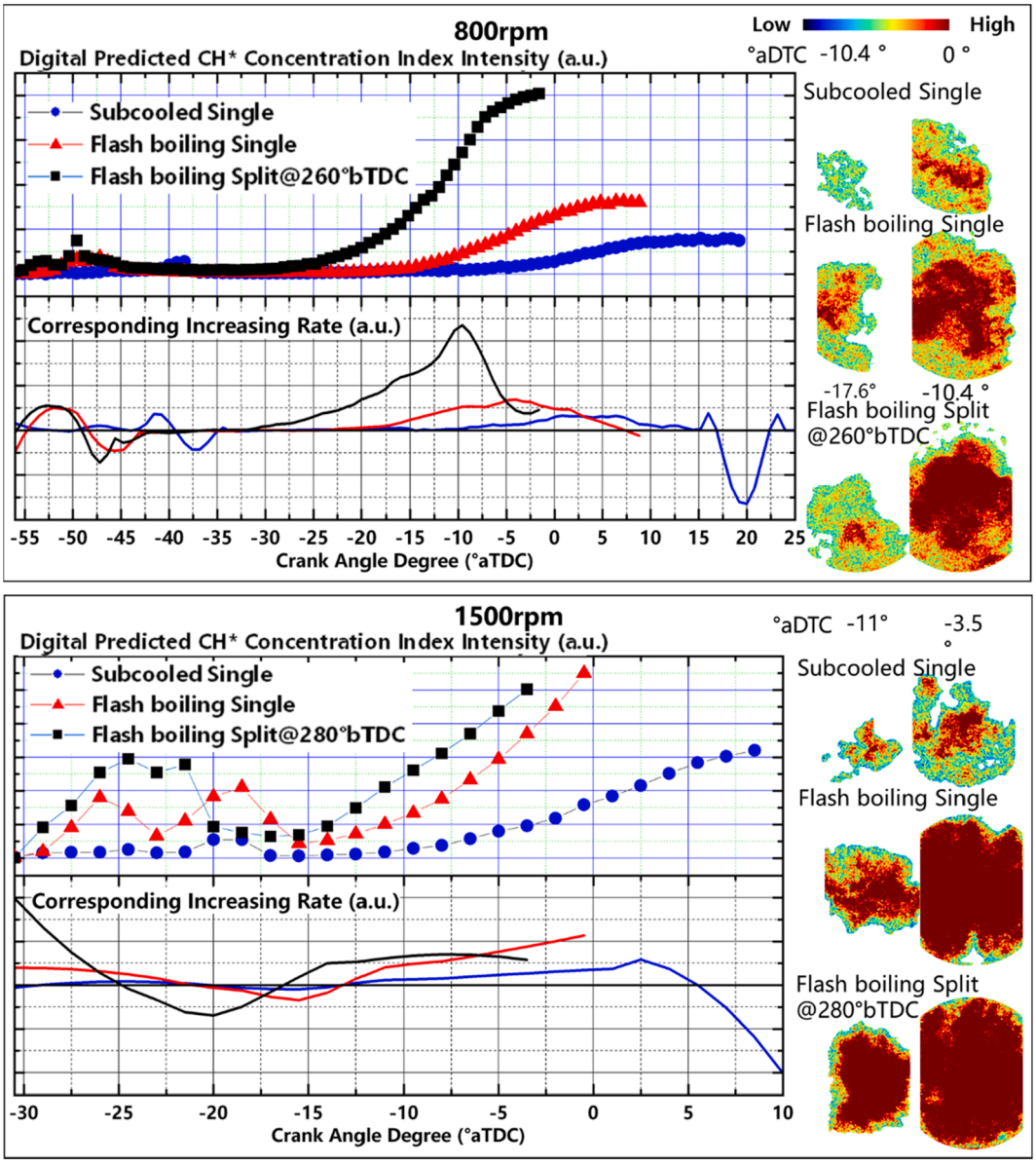

Fig. 14. Variation of digital CH* intensity under different injection timing, fuel temperature, and test speeds.

3.4. Discussion

Fig. 16 shows the variations between IMEP and CA50 for the 100 tested cycles under the conditions of a subcooled single, flash boiling single, and flash boiling multiple injections. At 800 rpm, the single injection subcooled and flash boiling cases have lower IMEP than the multiple flash boiling conditions. The single subcooled case has a delayed CA50, meaning the initial combustion speed is lower compared to that of the flash boiling case single case, while flash boiling multiple injections showed advanced CA50 compared to single injection cases. The cyclic variations in the single subcooled case were much higher since the variations of IMEP values are high. Several cycles with lower IMEP and delayed CA50 are highlighted by the circle in Fig. 16. These cycles represent a large number of incomplete combustion and even misfire cycles. This is attributed to the low-speed structure has low airflow intensity and slow flame propagation speed for single subcooled conditions, while flash boiling multiple and single conditions have fewer misfire cycles at the same engine operating parameters, which reflects the enhancement in mixture formation and flame development due to the flash boiling. Multiple flash boiling injection utilizes part of the injected fuel with the help of airflow to enhance the air–fuel mixing with lower loss of evaporation, so that improved the combustion performance (higher IMEP and advanced CA50). These results show that multiple injections are practical and improve combustion performance, especially for LBC during engine idle conditions. That returns to the difficulty of generating strong in-cylinder flow at the initial stage of the intake stroke, and the evaporation time for the fuel is also essential. Also, increasing the engine speed can develop more strong airflow, which eliminated these drawbacks.

At 1500 rpm, the IMEP of the type selected cases are in the order of flash boiling multiple > flash boiling single > subcooled single, while all cases showed the same range of CA50. The subcooled case showed the highest cyclic fluctuations at 1500 rpm compared to the flash boiling conditions, while the lowest IMEP showed the most retarded CA50. The flash boiling multiple improved the combustion and increased the IMEP at the lean combustion mode. It is challenging to solve the critical problems of IMEP in lean combustion mode using the traditional injection. Therefore, applying multiple injection flash boiling can enhance the fuel–air mixing capacity and change the heat release structure. This could contribute more to fast initial flame propagation and consequently

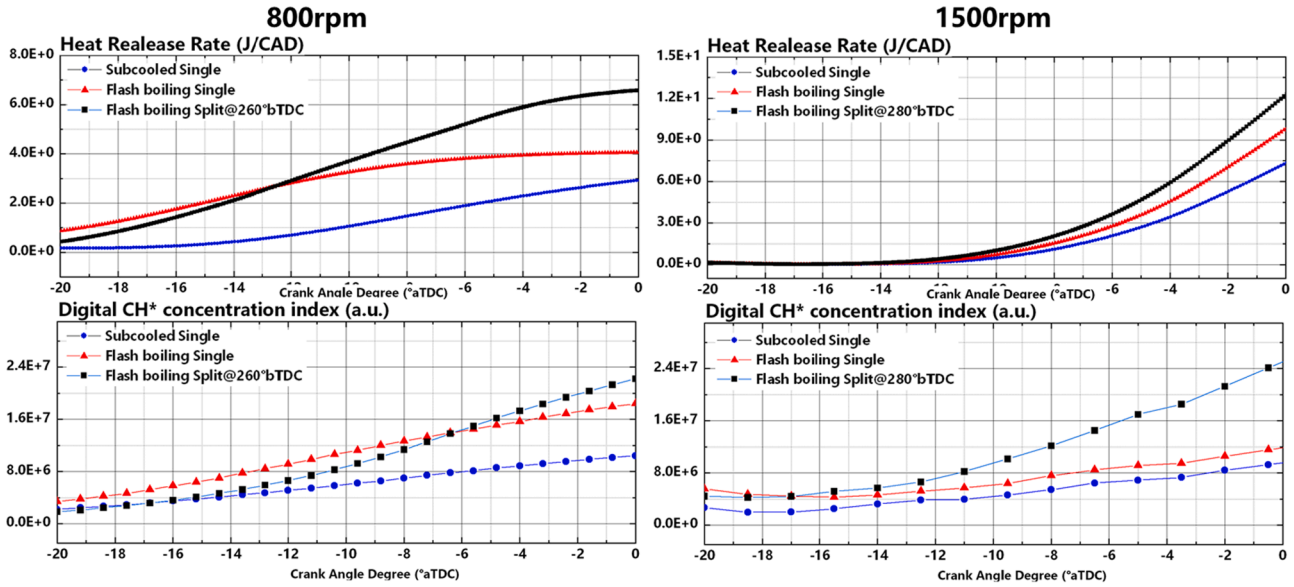

Fig. 15. Variation of CH* concentration and heat release rate under different injection timing, fuel temperature, and engine speed.

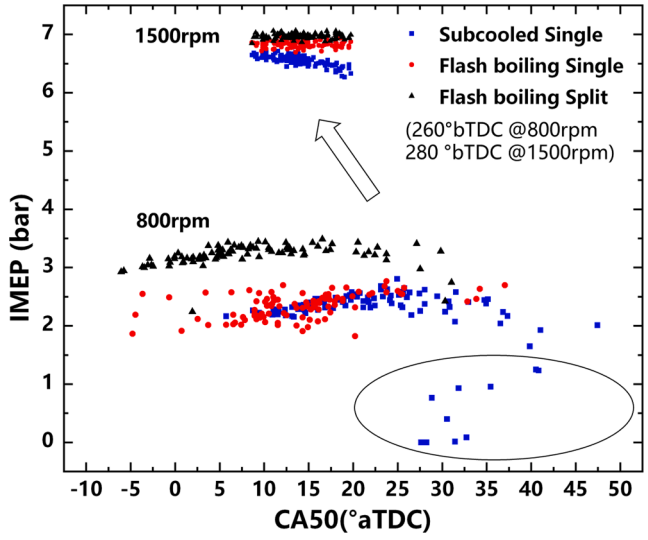

Fig. 16. Variations between IMEP and CA50 for 100 cycles under different injection timing, fuel temperature, and engine speed.

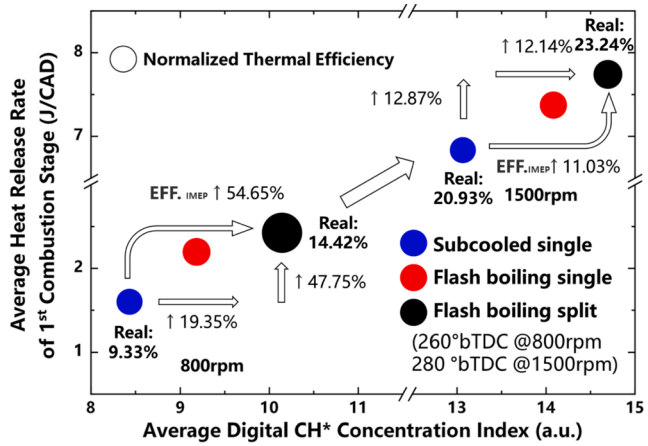

Fig. 17. Variation of fast burn stage versus the CH* concentration index.

higher IMEP. On the other hand, less cycle to cycle variation is essential in better engine performance. Therefore, flash boiling multiple injections achieved the best engine performance, as shown in Fig. 16.

Fig. 17 summarizes the variation of heat release rate during the fast burn mode, normalized thermal efficiency, and CH* concentration index. The circle size is correlated with the indicated thermal efficiency. At 800 rpm, the subcooled single injection case showed the lowest heat release, thermal efficiency, and CH* concentration. The flash boiling multiple injection case improved the heat release, thermal efficiency, and CH* concentration by 47.75%, 54.65%, and 19.35%, respectively, compared to the subcooled single injection case. The same trend is shown at 1500 rpm. The flash boiling multiple injection case improved the heat release, thermal efficiency, and CH* concentration by 12.87%, 11%, and 12.14%, respectively, compared to the subcooled single injection case. To conclude, the increase in thermal efficiency results from the rise in the heat release in the fast burn mode under the flash spray.

4. Conclusions

In this study, the flash boiling multiple injections is used to enhance the combustion of an optical direct injection spark ignition engine under lean operation ($\lambda = 1.55$) at 800 and 1500 rpm. A high-energy ignition system was used to ignite the lean fuel–air mixture. The second injection timing varied from 280 to 70 °bTDC to check the effect of tumble ratio variation during the cycle on the interaction of fuel and air. The Mie scattering technique was used for spray analyses. The in-cylinder airflow and tumble ratio variation across the cycle was investigated using CFD. A high-speed color camera filmed the flame through an optical quartz piston. A flame image postprocessing model was used to analyze the heat release features. The in-cylinder pressure was sampled and analyzed. The key results obtained from this study are summarized as follows:

- Flash boiling multiple injections enhances the fuel–air mixing as the fuel droplets quickly entrain the airflow field and mix with air. Mainly when the second injection is at the point of maximum tumble intensity, such as MF260 and MF280 at 800 rpm and 1500 rpm, respectively.
- Flash boiling spray can significantly reduce the high concentration of liquid droplets at the spray center, while the multiple spray strategy can dramatically reduce the wall wetting and quickly evaporate and mix to create a good mixture.

- Under high-energy ignition and lean combustion conditions, the fire nucleus of flash boiling spray combustion is faster, and the flame spreads faster, resulting in a shorter heat release process, increased heat release, and the overall combustion duration is short, which significantly improves thermal efficiency.
- The flash boiling multiple injection cases improved the heat release, thermal efficiency, and digital CH* concentration by 47.75%, 54.65%, and 19.35%, respectively, compared to the subcooled single injection case at 800 rpm. The same trend was shown at 1500 rpm and the flash boiling multiple injection case improved the heat release, thermal efficiency, and CH* concentration by 12.87%, 11%, and 12.14%.
- The flash boiling multiple injection cases with the second injection at the highest tumble ratio (MF280 at 1500 rpm and MF260 at 800 rpm) show the best combustion characteristics.

This paper proposes a method to use a multiple flash spray to optimize the combustion speed, improve the combustion stability, and improve the combustion efficiency in the low-speed lean combustion mode that requires high fuel–air mixing uniformity. This method is based on the characteristics of complete flash boiling spray and strong entrainment of the following flow and uses a control strategy to balance the evaporation time, wall wetting, and interaction with air, and maximizes the spray advantages of flash boiling spray, thereby optimizing combustion. The low Stokes number of the fuel droplets in the flash boiling spray makes the atomized fuel follow the airflow movement easily. Therefore, adjusting the injection timing at the point of the highest tumble intensity makes good use of this feature to promote air–fuel mixing. On the other hand, multiple injections can reduce the single injection duration and delay the second injection, thereby reducing piston wetting. Also, the rapid evaporation characteristics of flash boiling spray can prevent the deterioration caused by late injections. This method can be used technically to optimize future high-efficiency internal combustion engine combustion systems.

CRediT authorship contribution statement

Zhe Sun: . **:** Conceptualization, Methodology, Investigation, Project administration. **Qinglin Xu:** Writing - review & editing. **Mingli Cui:** Writing - review & editing. **Mohamed Nour:** Writing - original draft, Validation. **Xuesong Li:** Writing - review & editing. **David L.S. Hung:** Supervision. **Min Xu:** Project administration, Supervision.

Declaration of Competing Interest

The authors declare that they have no known competing financial interests or personal relationships that could have appeared to influence the work reported in this paper.

Acknowledgment

This research is sponsored by the National Natural Science Foundation of China (NSFC) under grant no. E52006140 and E51876126. It was carried out at the National Engineering Laboratory for Automotive Electronic Control Technology of Shanghai Jiao Tong University.

References

[1] Ratcliff MA, Burton J, Sindler P, Christensen E, Fouts L, Chupka GM, et al. Knock resistance and fine particle emissions for several biomass-derived oxygenates in a direct-injection spark-ignition engine. SAE Int J Fuels Lubr 2016;9(1):59–70. https://doi.org/10.4271/2016-01-0705.

[2] Costa M, Catapano F, Sementa P, Sorge U, Vaglieco BM. Mixture preparation and combustion in a GDI engine under stoichiometric or lean charge: an experimental and numerical study on an optically accessible engine. Appl Energy 2016;180:86–103. https://doi.org/10.1016/j.apenergy.2016.07.089.

[3] Su J, Xu M, Yin P, Gao Yi, Hung D. Particle number emissions reduction using multiple injection strategies in a boosted spark-ignition direct-injection (SIDI) gasoline engine. SAE Int J Engines 2015;8(1):20–9. https://doi.org/10.4271/2014-01-2845.

[4] Clark LG, Kook S, Chan QN, Hawkes E. The effect of fuel-injection timing on in-cylinder flow and combustion performance in a spark-ignition direct-injection (SIDI) engine using particle image velocimetry (PIV). Flow, Turbul Combust 2018;101(1):191–218. https://doi.org/10.1007/s10494-017-9887-x.

[5] Xu M, Zhang Y, Zeng W, Zhang G, Zhang M. Flash boiling : easy and better way to generate ideal sprays than the high injection pressure. SAE Int J Fuels Lubr 2013;6:137–48. https://doi.org/10.4271/2013-01-1614.

[6] Yang S, Li X, Hung DLS, Arai M, Xu M. In-nozzle flash boiling flow of multi-component fuel and its effect on near-nozzle spray. Fuel 2019;252:55–67. https://doi.org/10.1016/j.fuel.2019.04.104.

[7] Liu Yi, Pei Y, Peng Z, Qin J, Zhang Y, Ren Y, et al. Spray development and droplet characteristics of high temperature single-hole gasoline spray. Fuel 2017;191:97–105. https://doi.org/10.1016/j.fuel.2016.11.068.

[8] Shen S, Jia M, Wang T, Lü Q, Sun K. Measurement of the droplets sizes of a flash boiling spray using an improved extended glare point velocimetry and sizing. Exp Fluids 2016;57:1–16. https://doi.org/10.1007/s00348-016-2147-3.

[9] Xu Q, Pan H, Gao Y, Li X, Xu M. Investigation of two-hole flash-boiling plume-to-plume interaction and its impact on spray collapse. Int J Heat Mass Transf 2019;138:608–19. https://doi.org/10.1016/j.ijheatmasstransfer.2019.04.111.

[10] Wu S, Xu M, Hung DLS, Li T, Pan H. Near-nozzle spray and spray collapse characteristics of spark-ignition direct-injection fuel injectors under sub-cooled and superheated conditions. Fuel 2016;183:322–34. https://doi.org/10.1016/j.fuel.2016.06.080.

[11] Sun Z, Yang S, Nour M, Li X, Hung D, Xu M. Significant Impact of Flash Boiling Spray on In-Cylinder Soot Formation and Oxidation Process. Energy Fuels 2020;34(8):10030–8. https://doi.org/10.1021/acs.energyfuels.0c01942.

[12] Sun Z, Cui M, Nour M, Li X, Hung D, Xu M. Differences in pool-fire induced soot production between subcooled spray and flash boiling spray in a DISI engine. Fuel 2020:119453. doi: 10.1016/j.fuel.2020.119453.

[13] Sun Z, Cui M, Nour M, Li X, Hung D, Xu M. Differences in pool-fire induced soot production between subcooled spray and flash boiling spray in a DISI engine. Fuel 2020:119453. doi: 10.1016/j.fuel.2020.119453.

[14] Sun Z, Cui M, Nour M, Li X, Hung D, Xu M. Study of flash boiling combustion with different fuel injection timings in an optical engine using digital image processing diagnostics. Fuel 2021;284:119078. https://doi.org/10.1016/j.fuel.2020.119078.

[15] Sun Z, Cui M, Ye C, Yang S, Li X, Hung D, et al. Split injection flash boiling spray for high efficiency and low emissions in a GDI engine under lean combustion condition. Proc Combust Inst 2021;38(4):5769–79. https://doi.org/10.1016/j.proci.2020.05.037.

[16] Li Y, Guo H, Shen Y, Ma X, Chen L, Feng L. Macroscopic and microscopic characteristics of gasoline and butanol spray atomization under elevated ambient pressures. At Sprays 2018;28(9):779–95. https://doi.org/10.1615/AtomizSpr.v28.i910.1615/AtomizSpr.2018026194.

[17] Kale R, Banerjee R. Understanding spray and atomization characteristics of butanol isomers and isooctane under engine like hot injector body conditions. Fuel 2019;237:191–201. https://doi.org/10.1016/j.fuel.2018.09.142.

[18] Aleiferis PG, Van Romunde ZR. An analysis of spray development with iso-octane, n-pentane, gasoline, ethanol and n-butanol from a multi-hole injector under hot fuel conditions. Fuel 2013;105:143–68. https://doi.org/10.1016/j.fuel.2012.07.044.

[19] Serras-Pereira J, Aleiferis PG, Walmsley HL, Davies TJ, Cracknell RF. Heat flux characteristics of spray wall impingement with ethanol, butanol, iso-octane, gasoline and E10 fuels. Int J Heat Fluid Flow 2013;44:662–83. https://doi.org/10.1016/j.ijheatfluidflow.2013.09.010.

[20] Merola SS, Irimescu A, Tornatore C, Marchitto L, Valentino G. Split Injection in a DISI Engine Fuelled with Butanol and Gasoline Analyzed through Integrated Methodologies. SAE Int J Engines 2015;8(2):474–94. https://doi.org/10.4271/2015-01-0748.

[21] Sementa P, Maria Vaglieco B, Catapano F. Thermodynamic and optical characterizations of a high performance GDI engine operating in homogeneous and stratified charge mixture conditions fueled with gasoline and bio-ethanol. Fuel 2012;96:204–19. https://doi.org/10.1016/j.fuel.2011.12.068.

[22] Sun Z, Wang H, Cui M, Nour M, Li X, Xu M. Investigation of flash boiling injection schemes in lean-burn gasoline direct injection engines. Appl Energy Combust Sci 2021;7:100035. https://doi.org/10.1016/j.jaecs.2021.100035.

[23] Sun Z, Cui M, Wang H, Nour M, Li X, Xu M, et al. Effect of Split Injection Timing on Combustion and Emissions of a DISI Optical Engine Under Lean Burn Condition. Proc ASME 2020 Intern Combust Engine Div Fall Tech Conf ASME 2020 Intern Combust Engine Div Fall Tech Conf 2020:V001T03A007. doi: 10.1115/ICEF2020-2961.

[24] Sun Z, Li X, Nour M, Xu M. Investigation of flash boiling spray and combustion in SIDI engine under low-speed homogeneous lean operation. SAE Tech Pap 2021:1–9. https://doi.org/10.4271/2021-01-0467.

[25] Liu J, Dumitrescu CE. Methodology to separate the two burn stages of natural-gas lean premixed-combustion inside a diesel geometry. Energy Convers Manag 2019;195:21–31. https://doi.org/10.1016/j.enconman.2019.04.091.

[26] Liu J, Dumitrescu CE. Analysis of two-stage natural-gas lean combustion inside a diesel geometry. Appl Therm Eng 2019;160:114116. https://doi.org/10.1016/j.applthermaleng.2019.114116.

[27] Zizak G. Flame emission spectroscopy: fundamentals and applications 2000.

[28] Panoutsos C, Hardalupas Y, Taylor A. Numerical evaluation of equivalence ratio measurement using OH* and CH* chemiluminescence in premixed and non-premixed methane-air flames. Combust Flame 2009;156(2):273–91. https://doi.org/10.1016/j.combustflame.2008.11.008.

[29] Kathrotia T, Riedel U, Warnatz J. An experimental and numerical study on the adequacy of CH as a flame marker in premixed methane flames. Proc Combust Inst 2005;30:241–9. https://doi.org/10.1016/j.proci.2004.08.243.
[30] Han D, Fan Y, Sun Z, Nour M, Li X. Combustion and emissions of isomeric butanol / gasoline surrogates blends on an optical GDI engine. Fuel 2020;272:117690. https://doi.org/10.1016/j.fuel.2020.117690.
[31] Aleiferis PG, Serras-Pereira J, van Romunde Z, Caine J, Wirth M. Mechanisms of spray formation and combustion from a multi-hole injector with E85 and gasoline. Combust Flame 2010;157(4):735–56. https://doi.org/10.1016/j.combustflame.2009.12.019.
[32] Aleiferis PG, Malcolm JS, Todd AR, Cairns A, Hoffmann H. An optical study of spray development and combustion of ethanol, iso-octane and gasoline blends in a DISI engine. SAE Tech Pap 2008;2008:776–90. https://doi.org/10.4271/2008-01-0073.
[33] Xiao Di, Qiu S, Hung D, Li X, Nishida K, Xu M. Evaporation and condensation of flash boiling sprays impinging on a cold surface. Fuel 2021;287:119423. https://doi.org/10.1016/j.fuel.2020.119423.
[34] Nour M, Sun Z, Cui M, Yang S. Effect of flash boiling injection on combustion and PN emissions of DISI optical engine fueled with butanol. Proc Combust Inst 2021;38:5923–31. https://doi.org/10.1016/j.proci.2020.10.006.
[35] Ye C, Sun Z, Cui M, Li X, Hung D, Xu M. Ultra-lean limit extension for gasoline direct injection engine application via high energy ignition and flash boiling atomization. Proc Combust Inst 2021;38(4):5829–38. https://doi.org/10.1016/j.proci.2020.07.104.
[36] Kumar M, Shen T. In-cylinder pressure-based air-fuel ratio control for lean burn operation mode of SI engines. Energy 2017;120:106–16. https://doi.org/10.1016/j.energy.2016.12.091.
[37] Gong C, Li Z, Yi L, Liu F. Comparative study on combustion and emissions between methanol port-injection engine and methanol direct-injection engine with H2-enriched port-injection under lean-burn conditions. Energy Convers Manag 2019;200:112096. https://doi.org/10.1016/j.enconman.2019.112096.
[38] Jiang C, Wang C, Xu H, Liu H, Ma X. Engine performance and emissions of furan-series biofuels under stratified lean-burn combustion mode. Fuel 2021;285:119113. https://doi.org/10.1016/j.fuel.2020.119113.